Volume 45 | Number 37 | 7 October 2016 | Pages 14405–14816

Dalton Transactions

An international journal of inorganic chemistry

www.rsc.org/dalton

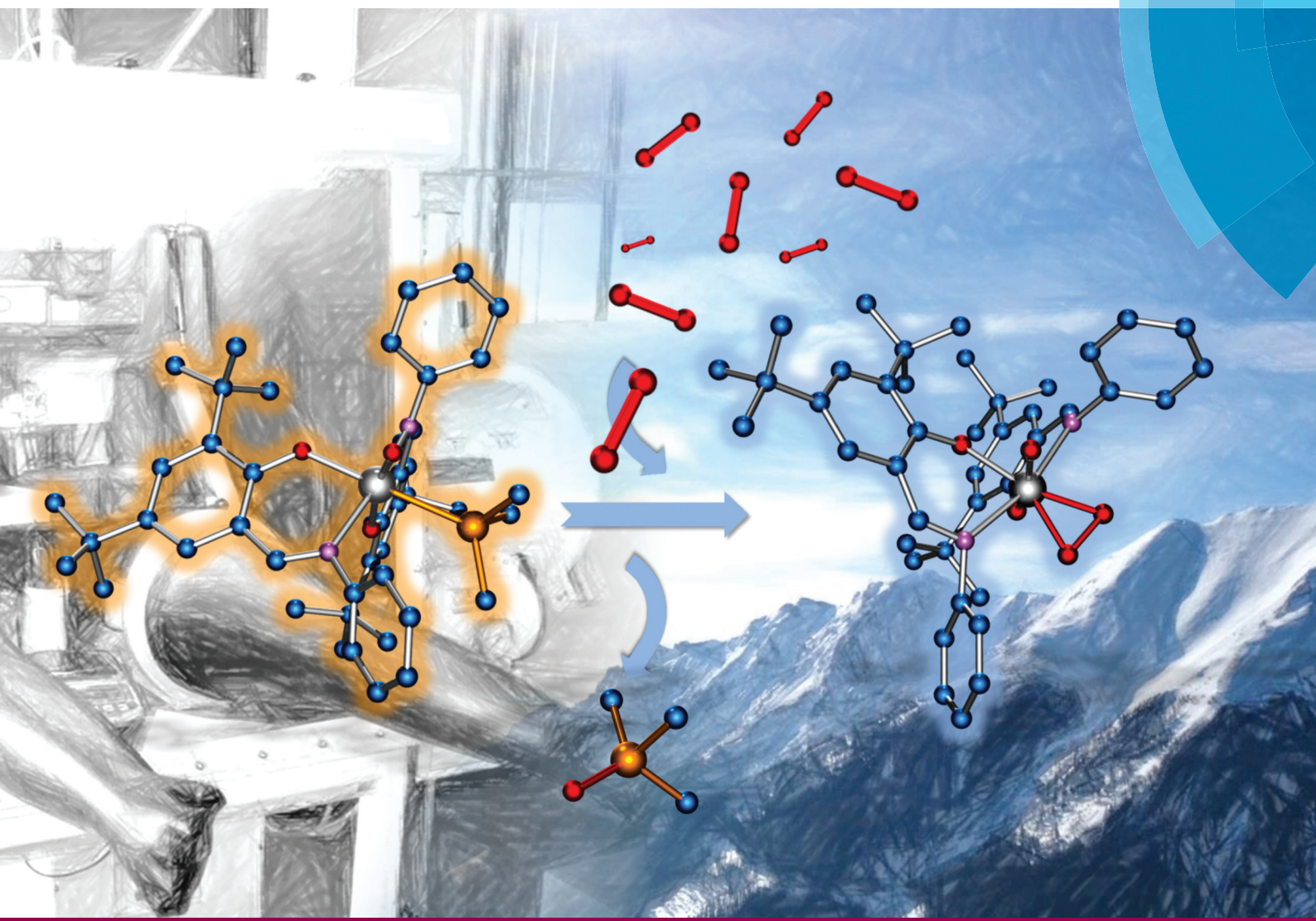

Themed issue: Small molecule activation

ISSN 1477-9226

ROYAL SOCIETY OF CHEMISTRY

PAPER

Nadia C. Mösch-Zanetti *et al.*

Oxygen activation and catalytic aerobic oxidation by Mo(IV)/(VI) complexes with functionalized iminophenolate ligands

175 YEARS

Dalton Transactions

PAPER

View Article Online
View Journal | View Issue

Cite this: *Dalton Trans.*, 2016, **45**, 14549

Oxygen activation and catalytic aerobic oxidation by Mo(IV)/(VI) complexes with functionalized iminophenolate ligands†

Niklas Zwettler, Martina E. Judmaier, Lara Strohmeier, Ferdinand Belaj and Nadia C. Mösch-Zanetti*

Received 29th April 2016,
Accepted 27th June 2016

DOI: 10.1039/c6dt01692h

www.rsc.org/dalton

Synthesis of molybdenum(VI) dioxido complexes **1–3**, coordinated by one or two functionalized iminophenolate ligands **HL1** or **HL2**, bearing a donor atom side chain or a phenyl substituent, respectively, allowed for systematic investigation of the oxygen atom transfer (OAT) reactivity of such complexes towards phosphanes. Depending on stoichiometry and employed phosphane (PMe_3 or PPh_3), different molybdenum(IV) and molybdenum(V) complexes **4–7** were obtained. Whereas molybdenum(IV) complexes **4** and **5**, bearing a terminal PMe_3 ligand, readily reacted with molecular O_2 to form oxido peroxido complexes **8** and **9**, phosphane free μ-oxido bridged dinuclear molybdenum(V) complexes **6** and **7** proved to be stable towards oxidation with molecular O_2 under ambient conditions. Single-crystal X-ray diffraction analyses revealed different isomeric structures in the solid state for dioxido complexes **1** and **2** in comparison with oxido phosphane complex **5**, dinuclear oxido μ-oxido complex **6** and oxido peroxido complexes **8** and **9**, pointing towards an isomeric rearrangement during OAT. Compounds **1** and **2** were furthermore tested for their ability to catalyze the aerobic oxidation of PMe_3 and PPh_3. A significant difference in catalytic activity has been observed in the oxidation of PMe_3, where complex **1** bearing donor atom functionalized ligands led to higher conversion and selectivity than complex **2** coordinated by phenyl iminophenolate ligands. In the oxidation of PPh_3, complex **2** leads to higher conversion compared to **1**. In a control experiment, phenyl-based dinuclear μ-oxido complex **7**, derived from complex **2**, was found to be catalytically active, which suggests a lower energy barrier for disproportionation into $[MoO(L)_2]$ and $[MoO_2(L)_2]$ in comparison with methoxypropylene based compound **6**, a prerequisite for subsequent reactivity toward molecular O_2.

Introduction

The chemistry of molybdenum, as an abundant and biologically relevant transition metal, has been well established over the course of the past few decades. Especially in biomimetic chemistry, much effort has been made to elucidate and mimic the structure and function of various molybdoenzymes.[1] An important class among these enzymes is represented by molybdenum oxotransferases such as DMSO reductase or xanthine oxidase, which contain a molybdenum(VI) metal center coordinated by an oxido ligand, as well as depending on the enzyme, one or two molybdopterin ligands.[2] These oxotransferases catalyze oxygen atom transfer reactions *via* a molybdenum(IV)/molybdenum(VI) redox cycle.[3] Whereas early modelling approaches for the corresponding active sites focused on sulfur rich dithiolene ligands, several other structurally diverse ligand systems have been explored.[3,4] The ease of such molybdenum compounds to undergo oxygen atom transfer made them also interesting in industrial applications. Especially for the catalytic oxidation of alkenes to epoxides, several highly efficient systems exist nowadays.[5]

In general, these catalysts use H_2O_2 or organic peroxides such as *tert*-butyl hydroperoxide (TBHP) as terminal oxidants. In our group, Mo(VI) dioxido systems were investigated for their applicability in oxygen atom transfer (OAT) reactions as well as epoxidation catalysis.[6–8,9] In that course, iminophenolate based complexes incorporating different functionalities were developed. While amides as internal hydrogen bond donors led to unprecedented C–C and C–N coupling behavior upon coordination,[10] the introduction of donor atoms (ether or amine) led to Mo(VI) catalysts for highly selective oxidation of a broad scope of alkene substrates with TBHP.[7]

Institute of Chemistry, Inorganic Chemistry, University of Graz, Schubertstrasse 1, 8010 Graz, Austria. E-mail: nadia.moesch@uni-graz.at

†Electronic supplementary information (ESI) available. CCDC 1476035–1476040 and 1486756. For ESI and crystallographic data in CIF or other electronic format see DOI: 10.1039/c6dt01692h

Nevertheless, one of the major drawbacks of to date reported catalysts is the necessity of a terminal oxidant. To develop more sustainable catalytic processes it is of great interest to allow for the use of molecular oxygen and in further consequence air as a benign alternative to other oxidants. Not only is oxygen abundant, cheap and environmentally harmless, its use also reduces the formation of undesired side products.[11] Whereas the activation of molecular oxygen has been described and thoroughly investigated for a variety of transition metals (*e.g.* iron, manganese),[12] the number of molybdenum complexes that activate molecular oxygen is very limited. Only a few examples with full structural characterization have been disclosed,[13,14] among them two examples are from our group.[15,16] In general there are only a few examples of homogeneously catalyzed aerobic oxidation reactions using a Mo catalyst and these are severely hampered by disadvantages such as high catalyst loadings or the need of a co-catalyst.[17]

Since the number of molybdenum oxido peroxido compounds originating from oxygen activation is scarce, it is important to gain further insight into the electronic and structural parameters affecting the applicability of Mo(IV)/Mo(VI) systems for oxygen atom transfer as well as oxygen activation. Our group has thus an ongoing research interest in the OAT and oxygen activation reactivity of Mo(IV)/Mo(VI) systems based on different iminophenolates, with special emphasis on the identification and unequivocal structural elucidation of all involved species to be able to predict and modify their reactivity. In further consequence this is beneficial for the development of systems for catalytic aerobic oxidation reactions.

Herein we present two new molybdenum(IV)/(VI) based systems coordinated by functionalized iminophenolate ligands. The chosen substituents are a methoxypropylene as well as a phenyl group. Whereas the donor functionality potentially acts as a "protection group" for vacant coordination sites, the phenyl group was chosen as an electron withdrawing substituent with steric demand, allowing for the comparison with a previously published system with electron donating *tert*-butyl substituents and thus electronic influences.[16] Two new molybdenum(VI) dioxido complexes employing these ligands were synthesized and investigated for their behavior in OAT reactions with the tertiary phosphanes PMe_3 and PPh_3 and subsequent reactivity towards molecular oxygen. Structural characterization *via* single-crystal X-ray diffraction analyses allowed assessing the isomeric structures of the participating species. Furthermore, catalytic oxidation of the phosphanes by molecular oxygen revealed significant reactivity differences depending on phosphanes and catalysts employed. Both investigated systems surpassed the PMe_3 conversion obtained using a previously published system.[16]

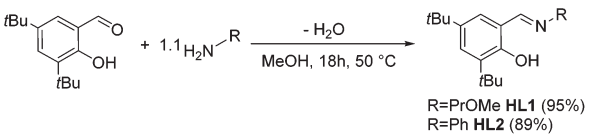

Scheme 1 Synthesis of the iminophenolate ligands **HL1** and **HL2**.

Results and discussion

Ligand synthesis

Previously published ligands **HL1** [18] and **HL2** [19] were prepared using well established synthetic protocols. Briefly, 1.1 equiv. of a primary amine bearing the desired functionality were added to a methanolic solution of 3,5-di-*tert*-butyl-2-hydroxy-benzaldehyde and stirred overnight at reflux temperature. Whereas **HL1** was obtained after evaporation of the solvent as a yellow oil, **HL2** was recovered as an orange crystalline solid after filtration (Scheme 1). Their analytic data is in agreement with the literature.[18,19]

Synthesis of molybdenum dioxido complexes

For the synthesis of molybdenum(VI) complexes of the type $[MoO_2(L)_2]$, synthetic procedures using $[MoO_2(acac)_2]$,[20] $[MoO_2Cl_2]$ and $[MoO_2Cl_2(DME)]$[21] (DME = dimethoxyethane) as metal sources were investigated.

A reaction of two equiv. of **HL1** and **HL2**, respectively, with the metal precursors $[MoO_2Cl_2(DME)]$ and $[MoO_2Cl_2]$ in the presence of excess NEt_3 in toluene, led to the targeted $[MoO_2(L)_2]$ complexes **1** and **2** in good yields (Scheme 2).

Generally, there are three possible isomers for molybdenum(VI) compounds with a *cis* dioxido arrangement coordinated by two iminophenolate ligands as depicted in Fig. 1. For complexes **1** and **2**, ^1H NMR data in C_6D_6 are consistent with the existence of two isomers in solution. One set of ligand resonances corresponds to isomer **A** as confirmed by single-crystal X-ray diffraction analysis. In principle also the O,O isomer **B** would feature one set of resonances but this would require a rotation of both ligands upon crystallization which seems highly unlikely. The non-equivalent ligand arrangement of the second isomer **C** in solution gives rise to two additional sets of ligand resonances. The ratio of the two isomeric forms is strongly dependent on

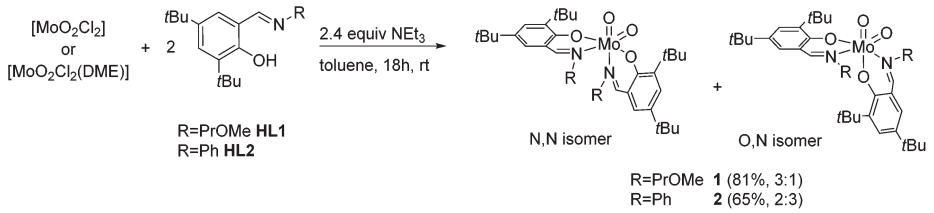

Scheme 2 Synthesis of molybdenum(VI) dioxido complexes **1** and **2** and their respective isomeric ratios (N,N : O,N).

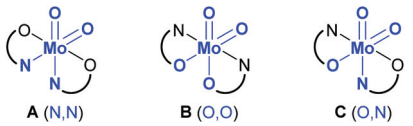

Fig. 1 Possible isomers **A–C** for a *cis* molybdenum(VI) dioxido complex coordinated by two iminophenolate ligands, and atoms *trans* to oxido groups in brackets.

the imine substituent. Whereas in the compound bearing the methoxypropylene-substituted ligands, the N,N form is predominant with a ratio of 3 : 1, in the complex with the phenyl-substituted ligand, the major isomer corresponds to the O,N form with a ratio of 2 : 3 (Scheme 2). In compound **1**, the signals for the minor isomer are considerably broadened, as previously observed,[7] whereas no significant broadening is observed in the ^{1}H NMR spectrum of **2** at room temperature.

Dissolution of single crystals of **2** and immediate recording of ^{1}H NMR spectra led to the same isomeric ratio in several attempts, suggesting a dynamic equilibrium in solution. Subsequent variable temperature ^{1}H NMR spectroscopy of complex **2** in C_6D_6 (Fig. S6†) showed a significant broadening of the O,N isomeric resonances upon heating accompanied by a slight change in the isomeric ratio (N,N : O,N approx. 2 : 3 at 9 °C to 5 : 6 at 50 °C). Similar results have been reported previously for a complex closely related to **1** (R = methoxyethylene).[7] A more pronounced effect can be observed in the ^{1}H NMR spectra of single crystals of **2** in different solvents (CD_3CN, CD_2Cl_2, Fig. S7†), where the isomeric N,N : O,N ratios are 1 : 1.2 (CD_2Cl_2) and 1.7 : 1 (CD_3CN), respectively, as recently observed for Re(V) iminophenolate complexes,[22] further corroborating a dynamic equilibrium in solution.

Upon using $[MoO_2(acac)_2]$ as a precursor, compound **1** was obtained in significant lower yield and compound **2** did not form. However, the monosubstituted complex $[MoO_2(acac)(L2)]$ (**3**) could be isolated in 34% yield which could not be improved with excess ligand (Scheme 3). NMR spectroscopy clearly features resonances for one iminophenolate and one acetylacetonate ligand.

The moisture sensitive complexes **1–3** are well soluble in most organic solvents including aliphatic hydrocarbons. Spectroscopic data (^{1}H, ^{13}C NMR and FT-IR spectroscopy), elemental analyses as well as single-crystal X-ray diffraction analyses confirm their structures.

OAT reactivity of complexes 1–3

The reaction of Mo(VI) dioxido compounds **1** or **2** with excess PMe_3 (5 equiv.) led to phosphane coordinated Mo(IV) oxido

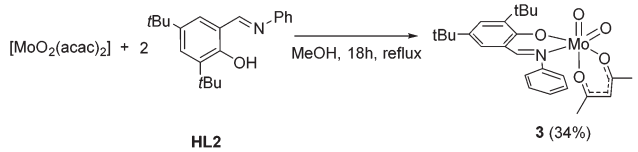

Scheme 3 Synthesis of monosubstituted complex **3**.

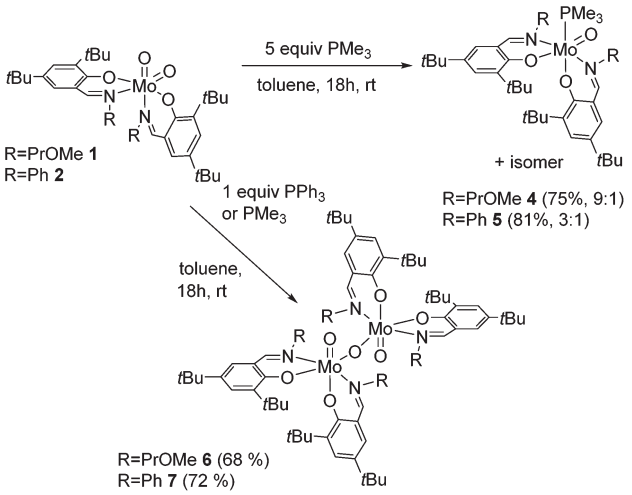

Scheme 4 OAT reactions of complexes **1** and **2** with PMe_3 and PPh_3 with isomeric ratios for complexes **4** and **5**. For clarity, only one possible isomer is depicted for all complexes.

compounds **4** and **5** in very good yields (Scheme 4). Similar to the ^{1}H NMR resonances for **1** and **2**, also for these oxido phosphane compounds two distinct species are observed in solution, reflected by two sets of resonances for two non-equivalent arranged ligands each. For both isomers, the coordinated PMe_3 molecule gives rise to a distinct resonance in the decoupled ^{31}P NMR spectra of **4** and **5**.

The isomeric ratios for the oxido phosphane complexes are found to be 9 : 1 (**4**) and 3 : 1 (**5**), thus revealing a significant shift in the isomeric ratio for **4** in comparison with **1** (ratio 3 : 1), whereas the isomeric ratio for **5** is in a similar range than for **2** (ratio 3 : 2). As all possible isomers exhibit non-equivalent ligand surroundings, routine NMR spectroscopy does not allow for the determination of specific isomers. However, we were able to obtain single-crystals suitable for X-ray diffraction analysis of **5**, which revealed it to be the O,O isomeric form (type **B**, Fig. 1) depicted in Scheme 4.

This is in contrast to the solid state structures of **1** and **2** which displayed the N,N isomeric form (type **A**, Fig. 1) and points towards an isomeric rearrangement during the transformation of **2** to **5**. The rearrangement is likely caused by higher steric demand of the phosphane ligand, which is corroborated by the exclusive O,O isomeric structure of a previously reported system featuring ligands with high steric demand (R = *t*Bu).[16] Dissolution of single crystals and immediate recording of a ^{1}H NMR spectrum showed an isomerically pure compound and allowed for the identification of the major isomer in solution as the O,O isomeric form. Interestingly, a ^{1}H NMR spectrum of the same sample after 24 h still showed only resonances corresponding to the O,O isomer, accompanied by traces of oxidized complex **9**. This suggests that the two isomers found for **5** are not in a dynamic equilibrium or equilibrate only slowly. Whereas similar unambiguous evidence *via* the solid state structure cannot be provided for compound **4**, we assume that it exhibits similar properties, especially due to

the observation of the O,O structural motif in the molecular structure of both corresponding oxido peroxido compounds **8** and **9** (*vide infra*).

The reactions of dioxido compounds **1** and **2**, respectively, with the more bulky PPh_3 or with stoichiometric amounts of PMe_3 led to species **6** and **7** in good yields (Scheme 4). Proton NMR spectroscopy reveals two sets of ligand resonances for **6** and **7** corresponding to a non-equivalent arrangement of the ligands, furthermore both compounds adopt a single isomer in solution. Neither **6** nor **7** shows any resonances in the ^{31}P NMR spectra and both are thus phosphane free. Single-crystal X-ray diffraction analysis of **6** identified the compound as a μ-oxido bridged dinuclear oxidomolybdenum(v) complex as shown in Scheme 4, complex **7** being likely of a similar structure. The reaction of the monosubstituted complex **3** with PMe_3 or PPh_3, respectively, led to the formation of several unidentified products.

Complexes **4** and **5** are very well and complexes **6** and **7** are well soluble in organic solvents including aliphatic hydrocarbons. Whereas **4** and **5** are highly sensitive towards air and moisture, **6** and **7** are stable towards air and traces of moisture. In solution, **4** and **5** tend to decompose within hours (**4**) to days (**5**). The compounds were characterized *via* ^1H, ^{13}C, ^{31}P NMR and FT-IR spectroscopy as well as elemental analyses, confirming their structures. Complexes **5** and **6** have additionally been characterized *via* single-crystal X-ray diffraction analysis (*vide infra*).

Activation of molecular dioxygen

Complexes **4** and **5** cleanly reacted with molecular dioxygen, indicated by a quick color change from red-brown to orange-red, to form oxido peroxido compounds **8** and **9** in excellent yields (Scheme 5). Compound **8** is alternatively accessible in a one-pot reaction from **1** *via* the addition of excess PMe_3 (1 M solution in toluene) and subsequent stirring overnight under an O_2 atmosphere, similar to a previously reported procedure.[16] Compounds **6** and **7** were virtually non-reactive toward molecular oxygen under ambient conditions.

Exposure of **6** and **7** to molecular oxygen at 80 °C led to the formation of a mixture of dioxido and oxido peroxido complexes **1**/**8** and **2**/**9**, respectively, accompanied by severe decomposition to free ligands and NMR inactive species. The reaction of **6** or **7** with O_2 requires a preceding disproportionation reaction forming Mo(IV)O (and Mo(VI)O_2), which is corroborated by the necessity of high temperatures and the resulting product mixture.

Whereas, in contrast to complexes **1**, **2**, **4** and **5**, compound **8** exists as single isomer in solution, as evidenced by ^1H and ^{13}C NMR spectroscopy, complex **9** also exists as a mixture of two isomers in solution in an approximate ratio of 4 : 1.

Similar to the solid state structure of **5**, both oxido peroxido compounds were identified as the O,O isomer (type **B**, Fig. 1) *via* single-crystal X-ray diffraction analysis. It is feasible to assign the O,O form to the structure of **8** also in solution because only a single isomer is observed. Dissolution of single crystals of **9** and immediate recording of a ^1H NMR spectrum showed only resonances for one species, which we thus also assign to the O, O isomer. Interestingly, a ^1H NMR spectrum of the same sample after 24 h revealed the initial isomeric ratio of 4 : 1 pointing towards a (slow) dynamic equilibrium as previously observed in molybdenum(IV) isocyanide complexes.[23] Comparing the structure of the oxido peroxido compounds **8** and **9** with previously published *cis* oxido peroxido complexes originating from O_2 activation, it is evident that the O,O isomeric form is the preferred conformation for such compounds in the solid state.[6,15,16] Complexes **8** and **9** are well soluble in most organic solvents and soluble in aliphatic hydrocarbons. Both complexes are stable towards air but sensitive towards moisture.

Catalytic oxidation of phosphanes

Complexes **1** and **2** were tested for their ability to catalyze the aerobic oxidation of phosphanes, namely trimethyl phosphane and triphenyl phosphane, according to Scheme 6. The conditions used were 1 mol% catalyst with an excess of dry O_2 gas (1.5 atm) in C_6D_6 at room temperature. Blank experiments under identical conditions but without catalysts led to conversions of PMe_3 and PPh_3 to <5%. In the aerobic oxidation of PMe_3, catalyst **1** was found to be significantly more active compared to **2** (65 *vs.* 35% conversion, Table 1) and more active than the previously described *tert*-butyl based system (19%).[16] Catalyst **2** proved to be unselective as only 25% of $OPMe_3$ was formed together with 10% of one side product. NMR spec-

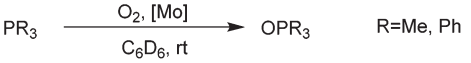

Scheme 6 Molybdenum(VI)-catalyzed aerobic oxidation of phosphanes, [Mo] = **1** or **2**.

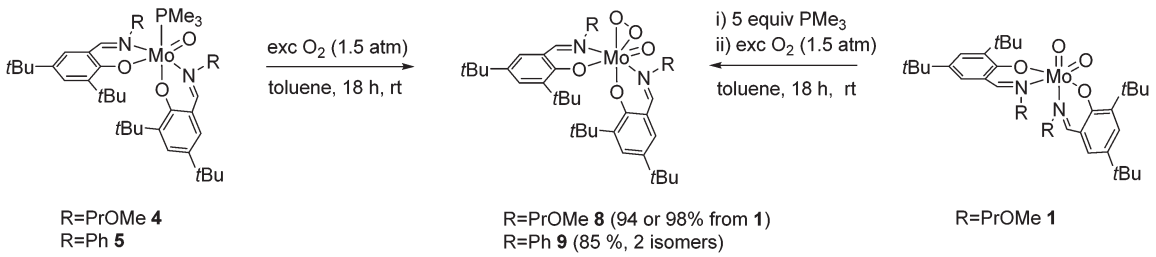

Scheme 5 Activation of molecular oxygen to form oxido peroxido compounds **8** and **9**.

Table 1 Yield of phosphane oxide after 24 h in the aerobic oxidation of phosphanes catalyzed by **1** or **2**

	1	**2**
PMe_3	65	25[a]
PPh_3	8 (3)[b]	23 (12)[b]

Conditions: 1 mol% catalyst, rt, C_6D_6. [a] 35% conversion of PMe_3. [b] Values in brackets correspond to dimeric molybdenum(v) μ-oxido complexes **6** and **7** as catalysts.

troscopy revealed it to be methyl dimethylphosphinate ($OP(OMe)Me_2$) where an additional oxygen atom was inserted into one P–C bond (Fig. S37 and 38†). This is highly interesting as it demonstrates for the first time the transfer of two oxygen atoms from a molybdenum oxido peroxido species to one substrate molecule.

In contrast, PPh_3 was oxidized selectively to $OPPh_3$ by **2**, but only 23% was converted. Interestingly, catalyst **1** was virtually non-reactive for the oxidation of PPh_3 (8%). To our further understanding of this reactivity difference, we subsequently tested the dimeric complexes **6** and **7** in the catalytic oxidation of PPh_3. Phenyl-based compound **7** led to a fourfold higher yield of $OPPh_3$ (12% *vs.* 3%) in comparison with methoxypropylene based complex **6**. This is in good agreement with the activity difference of **1** and **2** in the aerobic oxidation of PPh_3 and suggests lower activation energy for the disproportionation of **7**, a requirement for reactivity with O_2, in comparison with **6**. The temperature increase in the catalytic oxidation of PPh_3 was tested but due to significant autooxidation at 50 °C, as observed in a blank experiment, no reliable results could be obtained. To confirm the participation of the $[MoO(O_2)L_2]$ species in the catalytic oxidation, we reacted complex **9** with 2 equiv. of PMe_3 in a control experiment. Proton NMR measurement after 6 h of reaction time showed a mixture of **9** and the phosphane complex **5** together with $OPMe_3$ and residual PMe_3 but no dioxido species **2** (Fig. S45†). These results confirm the oxidation capability of complex **9** and are in good agreement with previous observations.[16]

Molecular structures

The molecular structures of molybdenum(vi) dioxido complexes **1–3**, molybdenum(iv) oxido phosphane complex **5**, molybdenum(v) oxido μ-oxido complex **6** as well as molybdenum(vi) oxido peroxido complexes **8** and **9** were determined by single-crystal X-ray diffraction analysis. The molecular views of **1–3** are given in Fig. 2, those of **5** and **6** in Fig. 3, and those of **8** and **9** in Fig. 4. Selected bond lengths and angles for com-

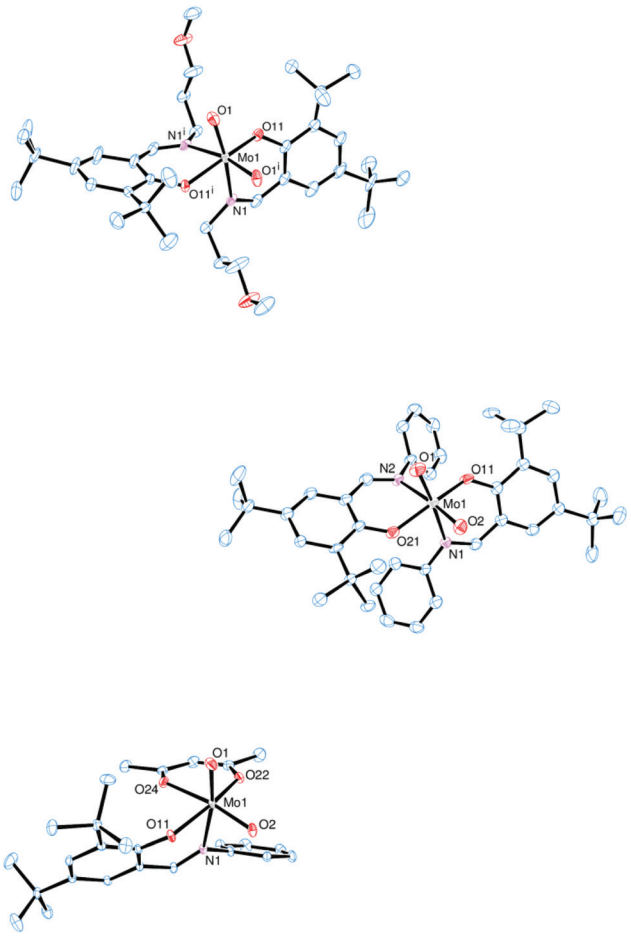

Fig. 2 Molecular views (50% probability level) of **1** (top), **2** (middle) and **3** (bottom); hydrogen atoms as well as solvent molecules are omitted for clarity.

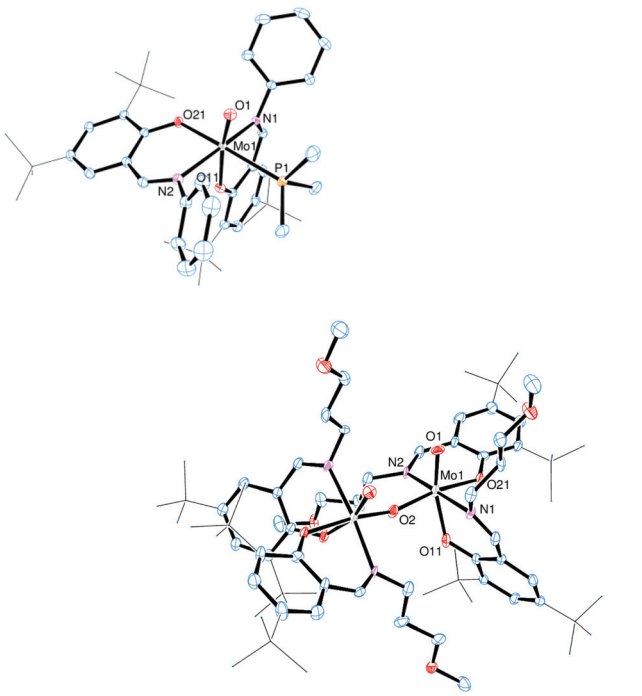

Fig. 3 Molecular views (50% probability level) of **5** (top), and **6** (bottom); hydrogen atoms as well as solvent molecules are omitted for clarity, and *tert*-butyl substituents are depicted as a wireframe. For disordered fragments, only atoms with the higher site occupation factors are depicted. In complex **6**, only atoms in the asymmetric unit are labelled.

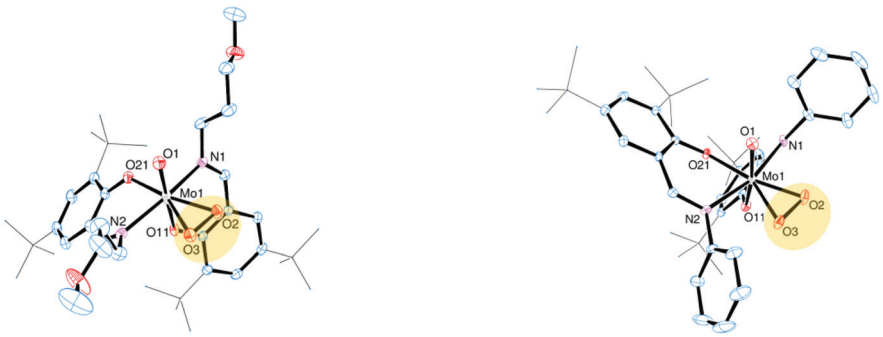

Fig. 4 Molecular views (50% probability level) of **8** (left) and **9** (right); hydrogen atoms as well as solvent molecules are omitted for clarity, and *tert*-butyl substituents are depicted as a wireframe. For disordered fragments, only atoms with the higher site occupation factors are depicted.

plexes **1–3**, **5**, **6**, **8** and **9** are provided in Table 2, and full crystallographic details such as structure refinement as well as experimental details are provided in the ESI.†

In complexes **1–3**, the molybdenum atoms are coordinated in a distorted octahedral fashion by two bidentate ligands and two terminal oxido ligands. In complexes **1** and **2**, which are coordinated by two iminophenolate ligands, the ligand arrangement corresponds to the N,N isomer (type **A**, Fig. 1) whereas in monosubstituted compound **3** one imine nitrogen as well as one acetylacetonate oxygen is *trans* to the oxido ligands. The molybdenum oxido bond lengths observed in **1–3** are within the expected ranges (Table 2).[24]

Compound **5**, which is obtained *via* OAT from **2** to PMe_3, is coordinated by two bidentate iminophenolate ligands, one terminal phosphane and one terminal oxido ligand in a distorted octahedral fashion. Interestingly, the arrangement of the iminophenolate ligands differs from the parent compound. In **5**, the phenolate oxygens are *trans* to the phosphane and oxido ligands, respectively, which correspond to the O,O isomer (type **B**, Fig. 1). The Mo=O bond length is 1.7037(13) Å and the Mo–P bond length is 2.5289(6) Å, thus both are rather long but comparable to previously structurally characterized molybdenum(IV) oxido phosphane complexes (Table 2).[8,25]

Compound **6**, obtained *via* OAT from **1** to PPh_3 displays a μ-oxido bridged dimeric structure with two molybdenum(V) oxido metal centers each coordinated by two bidentate ligands, a terminal oxido ligand as well as the μ-oxido ligand in a distorted octahedral fashion. The complex is symmetric around the bridging oxido ligand with a Mo1–O2–$Mo1^{i}$ angle of 157.2(5)° as well as twisted about the Mo1···Mo1′ connecting line (O1–Mo1···Mo1′–O1′ −31.1(3)°, N1–Mo1···Mo1′–N2′ −42.8(3)°), rendering the two terminal oxido ligands in a *gauche*-like conformation in the solid state. The arrangement of the ligands around the metal centers resemble the O,O isomer (Fig. 1) with the phenolate oxygens *trans* to the oxido and μ-oxido ligands, respectively. The Mo=O and Mo–(μ-O) bond lengths are within the expected ranges (Table 2).[24,26]

Compounds **8** and **9** are coordinated by two bidentate iminophenolate ligands, a terminal oxido ligand and a η^2 side-on coordinated peroxido ligand in a distorted octahedral fashion.

Both compounds adopt the O,O isomeric form in the solid state, with the phenolate oxygen atoms *trans* to the oxido and peroxido ligands, respectively. Whereas the Mo=O bond lengths for **8** and **9** as well as the Mo–O (peroxido) bond lengths in **9** are similar to previously reported Mo(VI) oxido peroxido compounds, the Mo–O (peroxido) distances in **8** are

Table 2 Selected bond lengths [Å] and angles [°] for complexes **1–3**, **5**, **6**, **8** and **9**

	1	**2**	**3** [a]	**5**	**6**	**8**	**9**
Mo1–O1	1.7099(11)	1.707(3)	1.7049(13)–1.7097(13)	1.7037(13)	1.694(6)	1.642(2)	1.6928(13)
Mo1–O2	1.7099(11)	1.706(3)	1.7028(13)–1.7109(13)	—	1.8883(18)[b]	1.981(2)	1.9581(13)
Mo1–O3	—	—	—	—	—	2.012(2)	1.9301(13)
Mo1–O11	1.9729(11)	1.946(3)	1.9243(12)–1.9304(13)	2.0660(14)	2.054(6)	2.0413(12)	2.0166(12)
Mo1–O21	1.9729(11)	1.946(2)	—	2.0816(11)	2.063(5)	2.0262(12)	2.0493(12)
Mo1–N1	2.3319(12)	2.375(3)	2.3974(15)–2.4021(15)	2.1272(13)	2.182(6)	2.1810(15)	2.2137(15)
Mo1–N2	2.3319(12)	2.394(3)	—	2.1769(13)	2.155(6)	2.1852(15)	2.1654(15)
O2–O3	—	—	—	—	—	1.430(3)	1.4425(18)
O1–Mo1–O2	107.82(8)	105.98(13)	104.17(6)–104.51(7)	—	100.5(3)	99.53(9)	100.97(6)
O1–Mo1–O3	—	—	—	—	—	100.03(9)	104.14(6)
O11–Mo1–O21	161.05(6)	152.33(11)	—	86.95(5)	79.9(2)	81.01(5)	77.09(5)
N1–Mo1–N2	75.13(6)	84.47(10)	—	164.99(5)	174.3(3)	160.74(5)	164.52(5)

[a] Bond length and angle range given due to four distinct molecules in the unit cell. [b] O2 = μ-oxido.

elongated with 2.012(2) and 1.981(2) Å as well as 2.132(5) and 2.056(5) Å for two disordered arrangements, respectively.[13,15,16]

From comparison of the bond lengths of the phenyl iminophenolate derived complexes **2**, **5**, **6** and **9**, it is evident that the different ligand arrangements in **2** (N,N isomer, type **A**, Fig. 1) as well as **5**, **6** and **9** (O,O type arrangement, Fig. 1) have a pronounced impact on the Mo–N bond lengths which are 2.375(3) and 2.394(3) Å in **2**, 2.1272(13) and 2.1769(13) Å in **5**, 2.182(6) and 2.155(6) Å in **6**, as well as 2.1654(15) and 2.2137(15) Å in **9**. The solid state structure thus reveals an elongation of the Mo–N bond lengths in the N,N isomeric structure found in **2** which is likely caused by the *trans* influence of the oxido ligands. A comparison of the Mo–O (phenolate) bond lengths in these complexes shows a comparable but opposite trend, *i.e.* an elongation of the Mo–O (phenolate) bonds in the molecular structures of **5**, **6** and **9**, again likely caused by the oxido *trans* influence. It can be thus further reasoned that the isomeric arrangement compared to the oxidation state of the metal center has a more significant impact on the metal–ligand bonding situation in these complexes.

Conclusions

The reaction of functionalized iminophenolate ligands with molybdenum(VI) metal precursors $[MoO_2Cl_2]$ and $[MoO_2Cl_2(DME)]$ yielded disubstituted complexes **1** and **2**, whereas the use of $[MoO_2(acac)_2]$ as a metal source led to monosubstituted complex **3** coordinated by one iminophenolate and one $acac^-$ moiety. Subsequent oxygen atom transfer from **1** or **2** to phosphanes gave rise to distinct molybdenum(IV) and molybdenum(V) complexes. The products obtained from the reactions of **1** and **2** were dependent on the nature of the phosphane (PMe_3 or PPh_3) as well as the employed stoichiometry. The use of excess of PMe_3 yielded molybdenum(IV) oxido phosphane complexes **4** and **5**. Upon the use of stoichiometric amounts of PMe_3 or PPh_3 molybdenum(V) μ-oxido complexes **6** and **7** were obtained. Compounds **4** and **5** readily reacted with molecular oxygen under ambient conditions to give oxido peroxido complexes **8** and **9**, while **6** and **7** did not show similar reactivity. Complexes **1**, **2**, **4**, **5** and **9** exist as isomeric mixtures in solution, but for **8** only one isomer is observed.

Furthermore **1** and **2** adopt a different ligand arrangement than **5**, **6**, **8** and **9** in the solid state. A comparison of Mo–N and Mo–O bond lengths within the solid state structures of **1**, **2**, **5**, **6**, **8** and **9** reveals a significant impact of the oxido *trans* influence on the bonding situation in these complexes. Dioxido molybdenum(VI) complexes **1** and **2** have been found to catalyze the aerobic oxidation of PMe_3 and PPh_3 with noteworthy reactivity differences depending on the nature of the ligand. In the oxidation of PMe_3, compound **1** was significantly more active and selective in comparison with **2**, however **2** marked the first example of a catalyst capable of transferring both peroxido oxygen atoms to one substrate molecule and thus partially oxidizing trimethyl phosphane to methyl dimethylphosphinate ($OP(OMe)Me_2$). In the catalytic aerobic oxidation of PPh_3, complex **1** proved to be virtually unreactive whereas complex **2** gave significant yields of $OPPh_3$. In the case of PMe_3 oxidation, the active site is coordinated by a substrate molecule. Thus, prior elimination of PMe_3 is necessary, occurring readily under O_2 which we have recently demonstrated.[16] This is not possible with the more bulky PPh_3 as evidenced by the formation of dinuclear μ-oxido bridged complexes in stoichiometric reactions. However catalysis experiments using these dimeric compounds **6** and **7** as catalysts in the oxidation of PPh_3 showed the phenyl-based dinuclear compound **7** exhibiting catalytic activity whereas **6** was completely inactive. This indicates lower activation energy for the disproportionation of **7**, which is required for the reaction with molecular O_2, in comparison with compound **6**. The results presented herein provide further understanding of the species involved in OAT reactions as well as oxygen activation with molybdenum(IV)/(VI) systems and also insight into the diverse effects of ligand functionalization on the reactivity of such systems.

Experimental section

General

Unless specified otherwise, experiments were performed under inert conditions using standard Schlenk equipment. Commercially available chemicals were purchased from Sigma-Aldrich and used as received. No further purification or drying operations have been performed. The metal precursors $[MoO_2(acac)_2]$[20] and $[MoO_2Cl_2(DME)]$[21] were synthesized according to known procedures. Solvents were purified *via* a Pure-Solv MD-4-EN solvent purification system from Innovative Technology, Inc. Methanol was refluxed over activated magnesium for at least 24 h and then distilled prior to use. The ^1H, ^{13}C and ^{31}P NMR spectra were recorded on a Bruker Optics instrument at 300/75/121 MHz. The peaks are denoted as singlet (s), broad singlet (bs), doublet (d), doublet of doublets (dd), triplet (t), pseudo-doublet ("d"), pseudo-triplet ("t") and multiplet (m). The used solvents and peak assignment are mentioned in the specific data sets. Resonances in ^{31}P NMR were referenced to phosphoric acid as an external standard. Electron impact mass spectroscopy (EI-MS) measurements have been performed with an Agilent 5973 MSD mass spectrometer with a push rod. ESI-MS as well as HR-MS (ESI^+) measurements were performed at the University of Graz, Department of Analytical Chemistry. ESI measurements were performed using an Agilent 1100 Series LCMSD (SL type), HR-MS (ESI^+) measurements were performed using a Thermo Scientific Q-Exactive mass spectrometer in positive ion mode, and the used solvent was acetonitrile. The peaks are denoted as cationic mass peaks, and the unit is the according ion mass/charge ratio. Solid samples for infrared spectroscopy were measured on a Bruker Optics ALPHA FT-IR Spectrometer. Liquid samples were recorded in benzene on a Bruker FT-MIR matrix MF *in situ* spectrometer using a glass fiber optic probe.

The IR bands are reported with wavenumber (cm^{-1}) and intensities (s, strong; m, medium; w, weak). All elemental analyses were performed at the Technical University of Graz, Institute of Inorganic Chemistry using a Heraeus Vario Elementar automatic analyzer.

X-ray diffraction analyses

Single-crystal X-ray diffraction analyses were performed on a BRUKER-AXS SMART APEX II diffractometer equipped with a CCD detector. All measurements were performed using monochromatized Mo K_α radiation from an Incoatec microfocus sealed tube at 100 K (*cf.* Table S1†). Absorption corrections were performed semi-empirical from equivalents. The structures were solved by direct methods (SHELXS-97)[27] and refined by full-matrix least-squares techniques against F^2 (SHELXL-2014/6).[27] CCDC 1476035–1476040 and 1486756 contain the supplementary crystallographic data for this paper. Full experimental details for single-crystal X-ray diffraction analyses of all compounds are provided in the ESI.†

Ligand synthesis

All ligands are stable towards air and moderately stable towards moisture. They can be stored in a desiccator over P_2O_5 for several weeks without decomposition.

Synthesis of (*E*)-2,4-di-*tert*-butyl-6-(((3-methoxypropyl)imino)methyl)phenol (HL1).[18] Ligand **HL1** was prepared following published procedures. In brief, 3-methoxy-1-propylamine (1.25 g, 14.0 mmol) was added to a solution of 3,5-di-*tert*-butyl-2-hydroxy-benzaldehyde (3.28 g, 14.0 mmol) in 50 mL of MeOH and the resulting yellow solution was stirred at reflux temperature overnight. The reaction solution was subsequently dried over $MgSO_4$ and the solvent was evaporated *in vacuo* to give **HL1** as a yellow oil (95%, 4.05 g). Analytical data is in compliance with the literature, and the ^{1}H NMR shifts in C_6D_6 as well as IR bands are given for the purpose of comparison.[18] ^{1}H NMR (300 MHz, C_6D_6, 25 °C) δ: 14.14 (bs, 1H, OH), 7.91 (s, 1H, CH═N), 7.53 (d, 1H, ArH), 6.97 (d, 1H, ArH), 3.36 (t, 2H, CH_2), 3.17 (t, 2H, CH_2), 3.06 (s, 3H, OMe), 1.69 (m, 2H, CH_2), 1.62 (s, 9H, *t*Bu), 1.32 (s, 9H, *t*Bu) ppm; IR (ATR, cm^{-1}) $\tilde{\nu}$: 1631 (s), 1440 (s), 1390 (m), 1361 (m), 1251 (m), 1173 (m), 1120 (s), 876 (w).

Synthesis of (*E*)-2,4-di-*tert*-butyl-6-((phenylimino)methyl)phenol (HL2).[19] Ligand **HL2** was prepared following published procedures. In brief, aniline (0.92 mL, 10.0 mmol) was added to a solution of 3,5-di-*tert*-butyl-2-hydroxy-benzaldehyde (2.34 g, 10.0 mmol) in 25 mL of MeOH and the resulting yellow solution was stirred at reflux temperature overnight. The reaction mixture was subsequently cooled to room temperature and filtered. The precipitate was dried *in vacuo* to yield **HL2** as an orange crystalline solid (89%, 2.75 g). Analytical data is in compliance with the literature, and the ^{1}H NMR shifts in C_6D_6 as well as IR bands are given for the purpose of comparison.[19] ^{1}H NMR (300 MHz, C_6D_6, 25 °C) δ: 14.14 (s, 1H, OH), 8.08 (s, 1H, CH═N), 7.64 (d, 1H, ArH), 7.11–6.90 (m, 6H, ArH), 1.68 (s, 9H, *t*Bu), 1.34 (s, 9H, *t*Bu) ppm; IR (ATR, cm^{-1}) $\tilde{\nu}$: 1605 (m), 1437 (m), 1361 (m), 929 (m), 901 (s), 878 (m), 794 (s), 568 (m), 448 (m).

Complex syntheses

All complexes are sensitive towards moisture; complexes **4** and **5** are additionally highly sensitive towards air. They can be stored in an N_2-filled glovebox for several weeks without decomposition.

Synthesis of $[MoO_2(L1)_2]$ (1). For the synthesis of **1**, 2 equiv. of **HL1** (460 mg, 1.50 mmol) were dissolved in a small portion of dry toluene and slowly added to a solution of 1 equiv. $[MoO_2Cl_2(DME)]$ (220 mg, 0.75 mmol) in the same solvent (5 mL). Subsequently 2.4 equiv. Et_3N (255 µl, 1.81 mmol) were added *via* syringe. The orange reaction mixture was stirred overnight and then filtered through a glass frit packed with Celite. The solvent was removed *in vacuo* to afford a waxy product which was thoroughly washed with cold dry pentane to obtain pure **1** as a bright yellow solid (81%, 450 mg). Crystals suitable for single-crystal X-ray diffraction analysis were obtained *via* recrystallization from a concentrated THF solution layered with pentane at room temperature. ^{1}H NMR (300 MHz, C_6D_6, 25 °C, N,N isomer) δ: 7.99 (s, 2H, CH═N), 7.71 (d, 2H, ArH), 7.09 (d, 2H, ArH), 3.63–3.58 (m, 4H, CH_2), 3.16–3.09 (m, 2H, CH_2), 303–2.99 (m, 2H, CH_2), 2.92 (s, 6H, OMe), 2.00–1.92 (m, 4H, CH_2), 1.29 (s, 18H, *t*Bu), 1.27 (s, 18H, *t*Bu) ppm; ^{13}C NMR (75 MHz, C_6D_6, 25 °C, N,N isomer) δ: 168.04 (CH═N), 160.98 (Ar–O), 142.08, 139.58, 129.74, 128.19 (HSQC), 122.19 (Ar), 69.48 (CH_2), 58.11 (OMe), 57.36 (CH_2), 35.65, 34.38 (q-*t*Bu), 31.60, 31.56 (*t*Bu), 31.30 (CH_2) ppm; IR (ATR, cm^{-1}) $\tilde{\nu}$: 1628 (s), 1559 (w), 1460 (w), 1247 (s), 1108 (s), 1047 (w), 913 (m), 902 (s), 841 (s), 751 (s), 549 (s); EI-MS (70 eV) *m*/*z*: 738.6 $[M]^+$; Anal. calcd for $C_{38}H_{60}MoN_2O_6$: C, 61.94; H, 8.21; N, 3.80; found: C, 61.62, H, 8.09; N, 3.78%.

Synthesis of $[MoO_2(L2)_2]$ (2). For the synthesis of **2**, 2 equiv. of **HL2** (311 mg, 1.01 mmol) were dissolved in a small portion of dry toluene and slowly added to a suspension of 1 equiv. $[MoO_2Cl_2]$ (100 mg, 0.51 mmol) in the same solvent (3 mL). Subsequently 2.4 equiv. Et_3N (168 µl, 1.21 mmol) were added *via* syringe. The dark red reaction mixture was stirred overnight whereupon a yellow solid was precipitated. The precipitate was washed twice with dry pentane, loaded onto a glass frit packed with Celite and eluted with dry Et_2O until the eluent turned colorless. The solution was evaporated and the residual waxy orange solid was recrystallized from dry MeCN at −35 °C to yield **2·MeCN** as a dark yellow microcrystalline solid (65%, 389 mg). Crystals suitable for single-crystal X-ray diffraction analysis were obtained *via* slow evaporation of a concentrated MeCN solution at −35 °C. ^{1}H NMR (300 MHz, C_6D_6, 25 °C, O, N isomer) δ: 7.68 (d, 1H, ArH), 7.66 (d, 1H, ArH), 7.56 (s, 1H, CH═N), 7.44–7.41 (m, 2H, ArH), 7.41 (s, 1H, CH═N), 7.20–7.16 (m, 1H, ArH), 7.09–7.00 (m, 1H, ArH), 6.90–6.75 (m, 7H, ArH), 6.44 (d, 1H, ArH), 1.70 (s, 9H, *t*Bu), 1.49 (s, 9H, *t*Bu), 1.26 (s, 9H, *t*Bu), 1.23 (s, 9H, *t*Bu); ^{1}H NMR (300 MHz, C_6D_6, N, N isomer) δ: 7.88 (s, 2H, CH═N), 7.58 (d, 2H, ArH), 7.09–7.00 (m, 4H, ArH), 6.90–6.75 (m, 8H, ArH), 1.37 (s, 18H, *t*Bu), 1.24 (s, 18H, *t*Bu); ^{13}C NMR (HSQC 300/75 MHz, C_6D_6, 25 °C, O,N

isomer, q-C obscured) δ: 170.13, 165.54 (CH═N), 131.70, 129.59, 129.26, 128.97, 128.08, 127.95, 126.55, 126.00, 125.72, 125.67, 125.54, 123.26, 123.18, 123.06 (Ar), 31.21, 31.20, 29.85, 29.69 (*t*Bu); ^{13}C NMR (HSQC 300/75 MHz, C_6D_6, 25 °C, N,N isomer, q-C obscured) δ: 169.00 (CH═N), 130.20, 128.91, 128.73, 128.58, 128.48, 123.33, 123.18 (Ar), 31.21, 29.82 (*t*Bu); IR (ATR, cm^{-1}) $\tilde{\nu}$: 2956 (s), 1611 (s), 1592 (m), 1559 (w), 1486 (w), 1437 (w), 1272 (m), 1253 (s), 1177 (s), 928 (w), 910 (s), 897 (s), 845 (m), 765 (m), 705 (w), 554 (w); EI-MS (70 eV) *m*/*z*: 746.6 $[M]^+$; Anal. calcd for $C_{38}H_{60}MoN_2O_6{\cdot}CH_3CN$: C, 67.25; H, 7.05; N, 5.35; found: C, 67.03, H, 7.01; N, 5.47%.

Synthesis of [MoO_2(acac)(L2)] (3). For the synthesis of **3**, 2 equiv. of **HL2** (380 mg, 1.23 mmol) were added to a suspension of 1 equiv. [MoO_2(acac)$_2$] in dry MeCN (5 mL). The resulting orange reaction solution was then stirred at 80 °C overnight and subsequently evaporated *in vacuo.* The resulting oily orange product was treated with dry pentane (10 mL) and sonicated. The supernatant was removed *via* cannula filtration and the yellow residue was washed twice with 5 mL of dry pentane. Recrystallization of the residue from dry MeCN yielded **3** as bright yellow crystals (34%, 121 mg). Crystals suitable for single-crystal X-ray diffraction analysis were obtained *via* slow evaporation of a concentrated MeCN solution at −35 °C. ^{1}H NMR (300 MHz, C_6D_6, 25 °C) δ: 7.71 (d, 1H, ArH), 7.65 (s, 1H, CH═N), 7.15–7.12 (m, 2H, ArH), 7.01–6.88 (m, 4H, ArH), 4.83 (s, 1H, CH), 1.65 (s, 9H, *t*Bu), 1.44 (s, 3H, Me), 1.26 (s, 9H, *t*Bu), 1.13 (s, 3H, Me) ppm; ^{13}C NMR (300 MHz, C_6D_6, 25 °C) δ: 195.26, 185.83 (C═O), 166.81 (CH═N), 159.17 (Ar–O), 152.24, 142.66, 140.51, 130.47, 129.36, 128.45, 126.23, 123.91, 121.96 (Ar), 103.55 (CH), 35.75, 34.42 (q-*t*Bu), 31.53, 30.09 (*t*Bu), 27.27, 24.90 (Me) ppm; IR (ATR, cm^{-1}) $\tilde{\nu}$: 2962 (m), 1605 (m), 1518 (m), 1362 (m), 1275 (m), 1250 (m), 1177 (m), 928 (s), 901 (s), 848 (s), 794 (m), 762 (s), 695 (m), 568 (s), 450 (s); EI-MS (70 eV) *m*/*z*: 537.3 $[M]^+$; Anal. calcd for $C_{26}H_{35}MoNO_5$: C, 58.32; H, 6.21; N, 2.62; found: C, 58.15, H, 6.04; N, 2.68%.

Synthesis of [MoO(PMe_3)(L1)$_2$] (4). For the synthesis of **4**, a solution of 1 equiv. of **1** (103 mg, 0.14 mmol) in dry toluene was treated with 5 equiv. PMe_3 (70 µl, 0.70 mmol) in toluene at room temperature. The reddish brown solution was stirred at room temperature for 1 h, whereupon the solvent was evaporated *in vacuo*. The crude residue was re-dissolved in little cold dry heptane and filtered through a glass frit packed with Celite. Evaporation of all volatiles gave **4** as a dark brown solid material (75%, 85 mg). ^{1}H NMR (300 MHz, C_6D_6, 25 °C, putative O,O isomer) δ: 8.12 (s, 1H, CH═N), 8.01 (s, 1H, CH═N), 7.51 (d, 1H, ArH), 7.40 (d, 1H, ArH), 7.13 (d, 1H, ArH), 7.02 (d, 1H, ArH), 4.39–4.14 (m, 3H, CH_2), 4.08–3.99 (m, 1H, CH_2), 3.49–3.26 (m, 4H, CH_2), 3.17 (s, 3H, OMe), 3.04 (s, 3H, OMe), 2.89–2.76 (m, 1H, CH_2), 2.63–2.34 (m, 2H, CH_2), 2.29–2.16 (m, 1H, CH_2), 1.36 (s, 9H, *t*Bu), 1.35 (s, 9H, *t*Bu), 1.34 (s, 9H, *t*Bu), 1.29 (s, 9H, *t*Bu), 0.92 (d, 9H, PMe_3) ppm; ^{13}C NMR (75 MHz, C_6D_6, 25 °C, putative O,O isomer) δ: 168.92 (CH═N), 166.04 (Ar–O), 163.00 (CH═N), 162.09 (Ar–O), 140.20, 138.49, 136.50, 136.34, 131.20, 129.96, 129.38, 127.45 (HSQC), 121.25, 121.17 (Ar), 71.06, 69.49, 68.81, 66.68, (CH_2), 58.33 (2× OMe), 35.62, 35.45, 34.24, 33.99 (q-*t*Bu), 33.30 (CH_2), 31.86, 31.77 (*t*Bu), 30.86 (CH_2), 30.10, 29.91 (*t*Bu), 16.53 (d, PMe_3) ppm; ^{31}P NMR (121 MHz, C_6D_6, 25 °C) δ: −3.17 (putative O,N isomer, Mo-PMe_3), −3.48 (putative O,O isomer, Mo–PMe_3) ppm; IR (FT-IR, benzene, cm^{-1}) $\tilde{\nu}$: 1612 (s), 1435 (s), 1311 (m), 1256 (s), 1120 (s), 952 (m), 918 (s), 837 (s), 746 (m). ESI-MS (50 V) *m*/*z*: 722.3 $[M - PMe_3]^+$; Anal. calcd for $C_{41}H_{69}MoN_2O_5P$: C, 61.79; H, 8.73; N, 3.52; found: C, 62.14; H, 8.76; N, 3.51%.

Synthesis of [MoO(PMe_3)(L2)$_2$] (5). For the synthesis of **5**, a solution of 1 equiv. **2** (100 mg, 0.13 mmol) in dry toluene was treated with 5 equiv. PMe_3 (70 µl, 0.65 mmol) in toluene at room temperature. The dark red-brownish solution was stirred at room temperature overnight, whereupon the solvent was evaporated *in vacuo*. The crude residue was re-dissolved in little cold dry heptane and filtered through a glass frit packed with Celite. Evaporation of all volatiles gave **5** as a dark red-brownish solid material (81%, 93 mg). Crystals suitable for single-crystal X-ray diffraction analysis were obtained *via* slow evaporation of a concentrated MeCN solution at −35 °C. ^{1}H NMR (300 MHz, C_6D_6, 25 °C, O,O isomer) δ: 8.11 (s, 1H, CH═N), 8.04 (s, 1H, CH═N), 7.84–7.81 (m, 2H, ArH), 7.69–7.66 (m, 2H, ArH), 7.58 (d, 1H, ArH), 7.42 (d, 1H, ArH), 7.23–7.18 (m, 3H, ArH), 7.11–7.05 (m, 3H, ArH), 6.95–6.90 (m, 2H, ArH), 1.42 (s, 9H, *t*Bu), 1.34 (s, 18H, *t*Bu), 1.33 (s, 9H, *t*Bu), 0.45 (d, 9H, PMe_3) ppm; ^{13}C NMR (75 MHz, C_6D_6, 25 °C, O,O isomer) δ: 170.14 (CH═N), 166.47 (Ar–O), 163.63 (CH═N), 163.08 (Ar–O), 160.20, 157.97, 140.84, 138.73, 136.91, 136.67, 131.89, 131.16, 130.59, 129.28 (2×), 128.65, 128.03 (2×, HSQC), 126.57, 125.92, 124.85 (2×), 123.69 (2×), 121.44, 120.73 (Ar), 35.67, 35.53, 34.28, 34.04 (q-*t*Bu), 31.82, 31.68, 30.15, 29.99 (*t*Bu), 15.39 (d, PMe_3) ppm; ^{31}P NMR (121 MHz, C_6D_6, 25 °C) δ: −0.77 (O,O isomer, Mo-PMe_3), −1.99 (putative O,N isomer, Mo-PMe_3) ppm; IR (ATR, cm^{-1}) $\tilde{\nu}$: 2949 (m), 1601 (m), 1587 (m), 1527 (m), 1485 (m), 1254 (m), 1165 (s), 953 (w), 927 (s), 866 (m), 764 (m), 704 (m), 694 (m), 637 (w), 523 (s), 448 (w); HR-MS (ESI^+) *m*/*z*: $[M]^+$ calcd for $C_{45}H_{61}MoN_2O_3P$: 806.3474, found: 806.3474; Anal. calcd for $C_{45}H_{61}MoN_2O_3P$: C, 67.15; H, 7.64; N, 3.48; found: C, 67.60; H, 7.43; N, 3.35%.

Synthesis of {[MoO(L1)$_2$]$_2$(µ-O)} (6). For the synthesis of **6**, a solution of 1 equiv. **1** (103 mg, 0.14 mmol) in dry toluene (3 mL) was treated with 2 equiv. of PMe_3 (29 µl, 0.28 mmol). The addition resulted in a quick color change from orange to dark red. The solution was stirred for 1 h at room temperature, subsequently the solvent was removed *in vacuo* whereupon the crude product was re-dissolved in cold dry heptane (5 ml) and filtered through a glass frit packed with Celite. After concentration of the solution to ~2 mL, inert column chromatography on basic aluminum oxide with dry ether/pentane (1 : 1) as the eluent was performed and the first red band was collected. Evaporation of the solvent gave **6** as a dark red solid (68%, 69 mg). For elemental analyses, the complex was recrystallized from dry CH_2Cl_2. Alternatively, complex **6** is accessible by OAT from complex **1** (100 mg, 0.14 mmol, 1 equiv.) to PPh_3 (37 mg, 0.14 mmol, 1 equiv.) in dry toluene (5 mL). After stirring for 24 h at room temperature, purification was followed the procedure described above. Residual traces of PPh_3 were first eluted from the basic aluminum oxide column with pentane.

The use of polymer-bound PPh_3 led to insoluble by-products and thus a simplified work-up procedure. Crystals suitable for single-crystal X-ray diffraction analysis were obtained by slow evaporation of a concentrated MeCN solution at −35 °C. ^{1}H NMR (300 MHz, C_6D_6, 25 °C) δ: 8.26 (s, 2H, CH═N), 8.10 (s, 2H, CH═N), 7.57 (d, 2H, ArH), 7.46 (d, 2H, ArH), 7.02 (d, 2H, ArH), 6.84 (d, 2H, ArH), 5.04–4.97 (m, 2H, CH_2), 4.62–4.52 (m, 2H, CH_2), 4.39–4.30 (m, 2H, CH_2), 3.69–3.60 (m, 2H, CH_2), 3.42–3.24 (m, 4H, CH_2), 3.11–3.05 (m, 2H, CH_2), 3.02 (s, 6H, OMe). 2.92 (s, 6H, OMe), 2.78–2.47 (m, 8H, CH_2), 2.10–1.92 (m, 2H, CH_2), 1.41 (s, 18H, *t*Bu), 1.31 (s, 18H, *t*Bu), 1.22 (s, 18H, *t*Bu), 1.19 (s, 18H, *t*Bu) ppm; ^{13}C NMR (75 MHz, C_6D_6, 25 °C) δ: 169.91, 169.31 (CH═N), 166.94, 162.57 (Ar–O), 140.01, 139.28, 138.48, 137.47, 131.62, 129.96, 129.69, 128.85, 121.95, 121.87 (Ar), 70.26, 70.08, 61.30, 60.77 (CH_2), 58.35, 58.20 (OMe), 35.51, 35.23, 34.15, 33.99 (q-*t*Bu), 33.25, 31.95 (CH_2), 31.72, 31.44, 29.81, 29.46 (*t*Bu) ppm; IR (ATR, cm^{-1}) $\tilde{\nu}$: 1611 (s), 1597 (s), 1256 (s), 1104 (br, s), 1014 (br, s), 928 (s), 798 (br, s), 529 (s); EI-MS (70 eV) *m*/*z*: 722.6 $[MoO(L1)_2]^+$; Anal. calcd for $C_{76}H_{124}Mo_2N_4O_{10}{\cdot}CH_2Cl_2$: C, 59.80; H, 8.21; N, 3.62; found: C, 59.94; H, 8.40; N, 3.33%.

Synthesis of {[MoO(L2)$_2$]$_2$(μ-O)} (7). For the synthesis of **7**, 1 equiv. of **2** (100 mg, 0.13 mmol) and 1 equiv. of PPh_3 (34 mg, 0.13 mmol) were dissolved in dry MeCN (5 mL). The initially orange reaction solution was stirred at room temperature for 48 h whereupon it gradually darkened. The precipitate was subsequently filtered off, washed twice with little cold dry MeCN and dried *in vacuo*. After subsequent removal of the residual traces of PPh_3 and $OPPh_3$ *via* sublimation (110 °C, 2 × 10^{-5} atm), **7** was obtained as a dark purple solid (72%, 69 mg). The use of polymer-bound PPh_3 led to insoluble by-products and thus a simplified work-up procedure. ^{1}H NMR (300 MHz, C_6D_6, 25 °C) δ: 8.14–8.12 (m, 4H, ArH), 8.02 (s, 2H, CH═N), 7.63 (d, 2H, ArH), 7.55 (d, 2H, ArH), 7.43 (s, 2H, CH═N), 7.41–7.36 (m, 6H, ArH), 7.09–6.99 (m, 10H, ArH), 6.88 (d, 2H, ArH), 6.55 (d, 2H, ArH), 1.36 (s, 18H, *t*Bu), 1.26 ("d", 36H, *t*Bu), 1.20 (s, 18H, *t*Bu) ppm; ^{13}C NMR (75 MHz, C_6D_6, 25 °C) δ: 172.09, 169.54 (CH═N), 162.91, 161.76 (Ar–O), 157.25, 155.04, 140.88, 140.52, 139.39, 139.37, 131.00, 130.72, 130.43, 130.16, 128.09 (3×, HSQC), 127.97 (2×, HSQC), 126.82, 126.31 (2×), 126.05 (2×), 122.76, 120.69 (Ar), 35.70, 35.49, 34.27, 34.01 (q-*t*Bu), 31.79, 31.50, 30.52, 30.11 (*t*Bu) ppm; IR (ATR, cm^{-1}) $\tilde{\nu}$: 1618 (m), 1434 (m), 1250 (s), 1168 (s), 928 (m), 835 (s), 703 (s), 693 (s), 532 (vs); HR-MS (ESI$^+$) *m*/*z*: $[M]^+$ calcd for $C_{84}H_{104}Mo_2N_4O_7$: 1476.6013, found: 1476.6056; Anal. calcd for $C_{84}H_{104}Mo_2N_4O_7$: C, 68.46; H, 7.11; N, 3.80; found: C, 68.25; H, 6.80; N, 3.71%.

Synthesis of [MoO(O$_2$)(L1)$_2$] (8). For the synthesis of **8**, a solution of **4** (86 mg, 0.11 mmol) in dry toluene (3 mL) was treated with excess dry O_2 gas whereupon the initially dark brown solution quickly turned orange-red. The solution was stirred under an O_2 atmosphere (1.5 atm) overnight at room temperature. Subsequently all volatiles were removed *in vacuo*. The resulting dark orange residue was dissolved in a minimum amount of cold dry heptane and the resulting suspension was filtered through a glass frit packed with Celite. After evaporation *in vacuo*, **8** was obtained as an orange solid (94%, 76 mg). For elemental analyses, the complex was recrystallized from dry CH_2Cl_2. Single crystals suitable for X-ray diffraction analysis were obtained from concentrated THF solutions layered with pentane at room temperature. Alternatively, **8** is accessible directly from **1**. Thus 1 equiv. of **1** (0.14 mmol, 103 mg) was dissolved in dry toluene (5 mL). After addition of 5 equiv. of PMe_3 in toluene (0.70 mmol, 0.7 mL 1 M solution), the reaction solution was stirred under an O_2 atmosphere (1.5 atm) overnight at room temperature. The orange reaction mixture was subsequently evaporated to dryness, cold dry heptane (5 mL) was added and residual $OPMe_3$ was removed *via* filtration through a glass frit packed with Celite. After evaporation *in vacuo*, **8** was obtained as a brown-orange solid (98%, 103 mg). ^{1}H NMR (300 MHz, C_6D_6, 25 °C) δ: 8.27 (s, 1H, CH═N), 8.18 (s, 1H, CH═N), 7.63 (d, 1H, ArH), 7.47 (d, 1H, ArH), 7.03 (d, 1H, ArH), 6.98 (d, 1H, ArH), 5.25–5.17 (m, 1H, CH_2), 5.01–5.94 (m, 1H, CH_2), 4.22–4.08 (m, 2H, CH_2), 3.59–3.52 (m, 1H, CH_2), 3.35–3.19 (m, 3H, CH_2), 3.04 (s, 3H, OMe), 3.01 (s, 3H, OMe), 2.60–2.29 (m, 4H, CH_2), 1.32 (s, 9H, *t*Bu), 1.24 (s, 18H, *t*Bu), 1.15 (s, 9H, *t*Bu) ppm; ^{13}C NMR (75 MHz, C_6D_6, 25 °C) δ: 169.00, 168.35 (CH═N), 162.21, 160.64 (Ar–O), 139.70, 139.26, 139.06, 132.20, 130.67, 129.61, 129.28, 129.00, 121.93, 121.66 (Ar), 69.47, 69.39, 63.76, 59.68 (CH_2), 58.22, 58.19 (OMe), 35.06, 34.94 (q-*t*Bu), 34.15 (2× q-*t*Bu), 31.77 (CH_2), 31.60 (*t*Bu), 31.53 (CH_2), 31.48, 29.73, 29.56 (*t*Bu) ppm; IR (ATR, cm^{-1}) $\tilde{\nu}$: 1612 (s), 1256 (s), 1108 (br, s), 1089 (br, s), 914 (s), 839 (s), 800 (s), 779 (s), 748 (m), 539 (s); ESI-MS (100 V) *m*/*z* : 755.3 $[M]^+$; Anal. calcd for $C_{38}H_{60}MoN_2O_7{\cdot}0.2CH_2Cl_2$: C, 59.60; H, 7.91; N, 3.64; found: C, 59.26; H, 7.99; N, 4.00%.

Synthesis of [MoO(O$_2$)(L2)$_2$] (9). For the synthesis of **9**, a solution of **5** (100 mg, 0.12 mmol) in dry toluene (3 mL) was treated with excess dry O_2 gas whereupon the initially red-brown solution quickly turned deep orange. The solution was stirred under an O_2 atmosphere (1.5 atm) overnight at room temperature. Subsequently all volatiles were removed *in vacuo*. The resulting waxy dark orange residue was dissolved in a minimum amount of cold dry heptane and the resulting suspension was filtered through a glass frit packed with Celite. Evaporation of all volatiles *in vacuo* and subsequent sublimation of residual $OPMe_3$ traces (60 °C, 2 × 10^{-5} atm) gave **7** as a dark orange solid (85%, 84 mg). ^{1}H NMR (300 MHz, C_6D_6, 25 °C, O,O isomer) δ: 8.11 (s, 1H, CH═N), 8.10 (s, 1H, CH═N), 7.89–7.85 (m, 2H, ArH), 7.70 (d, 1H, ArH), 7.61–7.56 (m, 2H, ArH), 7.54 (d, 1H, ArH), 7.24–7.18 (m, 2H, ArH), 7.13–6.99 (m, 4H, ArH), 6.90 (d, 1H, ArH), 6.86 (d, 1H, ArH), 1.37 (s, 9H, *t*Bu), 1.26 (s, 9H, *t*Bu), 1.25 (s, 9H, *t*Bu), 1.23 (s, 9H, *t*Bu) ppm; ^{13}C NMR (HSQC 300/75 MHz, C_6D_6, 25 °C, q-C obscured) δ: 169.10, 168.74 (CH═N), 133.20, 131.41, 130.24, 129.74, 128.81, 128.48, 128.46, 128.09, 127.15, 126.90, 125.44, 125.26 (Ar), 124.74 (2× Ar), 31.19, 31.09, 29.64, 29.54 (*t*Bu); IR (ATR, cm^{-1}) $\tilde{\nu}$: 2953 (m), 1611 (s), 1589 (s), 1540 (m), 1252 (s), 1172 (s), 927 (s), 838 (s), 765 (m), 704 (m), 692 (m), 538 (br s); HR-MS (ESI$^+$) *m*/*z*: $[M + Na]^+$ calcd for $C_{42}H_{52}MoN_2NaO_5$: 785.2828, found: 785.2820; Anal. calcd for

$C_{42}H_{52}MoN_2O_5$: C, 66.30; H, 6.89; N, 3.68; found: C, 65.81; H, 7.05; N, 3.66%.

Catalytic aerobic oxidation of phosphanes

In a representative reaction, 5 mg of the respective catalyst (approx. 0.007 mmol) was dissolved in dry C_6D_6 under a N_2 atmosphere in a 50 mL Schlenk flask. Subsequently 100 equiv. of the respective phosphane (0.7 mmol PMe_3: 53 mg; PPh_3: 184 mg) were added to the solution. The Schlenk flask was then flushed with dry O_2 and placed under O_2 pressure (1.5 atm) whereupon the reaction solution was stirred for 24 h at room temperature. Subsequently the Schlenk flask was cooled to 0 °C and twice evacuated and backfilled with dry N_2. After addition of 0.2 mL of dry CD_3CN to ensure complete dissolution of all formed products, the reaction was monitored *via* ^1H and ^{31}P NMR spectroscopy, phosphane oxide yields were calculated *via* integration of the respective peak areas in the ^1H NMR spectra, and conversion included the peak areas for the formed side product ($OP(OMe)Me_2$ ^1H NMR in C_6D_6 δ: 3.34 (d, 3H, OMe), 1.08 (d, 6H, 2× Me); ^{31}P NMR in C_6D_6 δ: 49.93). Blank experiments without catalysts were included for both phosphanes, where yields of <5% were observed for PMe_3 and PPh_3.

Acknowledgements

Financial support by the Austrian Science Fund (FWF) (grant number P26264) and NAWI Graz is gratefully acknowledged.

References

1 (*a*) C. G. Young, in *Biomimetic Oxidations Catalyzed by Transition Metal Complexes*, ed. B. Meunier, World Scientific, Singapore, 2000, pp. 415–459; (*b*) S. Groysman and R. H. Holm, *Biochemistry*, 2009, **48**, 2310–2320.
2 (*a*) F. J. Hine, A. J. Taylor and C. D. Garner, *Coord. Chem. Rev.*, 2010, **254**, 1570–1579; (*b*) P. Basu and S. J. Burgmayer, *Coord. Chem. Rev.*, 2011, **255**, 1016–1038; (*c*) R. Hille, J. Hall and P. Basu, *Chem. Rev.*, 2014, **114**, 3963–4038.
3 K. Heinze, *Coord. Chem. Rev.*, 2015, **300**, 121–141.
4 (*a*) R. H. Holm, E. I. Solomon, A. Majumdar and A. Tenderholt, *Coord. Chem. Rev.*, 2011, **255**, 993–1015; (*b*) A. Majumdar and S. Sarkar, *Coord. Chem. Rev.*, 2011, **255**, 1039–1054.
5 S. A. Hauser, M. Cokoja and F. E. Kühn, *Catal. Sci. Technol.*, 2013, **3**, 552–561.
6 G. Lyashenko, G. Saischek, M. E. Judmaier, M. Volpe, J. Baumgartner, F. Belaj, V. Jancik, R. Herbst-Irmer and N. C. Mösch-Zanetti, *Dalton Trans.*, 2009, 5655–5665.
7 M. E. Judmaier, C. Holzer, M. Volpe and N. C. Mösch-Zanetti, *Inorg. Chem.*, 2012, **51**, 9956–9966.
8 M. Volpe and N. C. Mösch-Zanetti, *Inorg. Chem.*, 2012, **51**, 1440–1449.
9 (*a*) J. A. Schachner, P. Traar, C. Sala, M. Melcher, B. N. Harum, A. F. Sax, M. Volpe, F. Belaj and N. C. Mösch-Zanetti, *Inorg. Chem.*, 2012, **51**, 7642–7649; (*b*) M. E. Judmaier, C. H. Sala, F. Belaj, M. Volpe and N. C. Mösch-Zanetti, *New J. Chem.*, 2013, **37**, 2139; (*c*) A. Dupé, M. K. Hossain, J. A. Schachner, F. Belaj, A. Lehtonen, E. Nordlander and N. C. Mösch-Zanetti, *Eur. J. Inorg. Chem.*, 2015, 3572–3579; (*d*) N. C. Mösch-Zanetti, D. Wurm, M. Volpe, G. Lyashenko, B. Harum, F. Belaj and J. Baumgartner, *Inorg. Chem.*, 2010, **49**, 8914–8921.
10 N. Zwettler, A. Dupé, J. A. Schachner, F. Belaj and N. C. Mösch-Zanetti, *Inorg. Chem.*, 2015, **54**, 11969–11976.
11 *Modern Oxidation Methods*, ed. J.-E. Bäckvall, Wiley-VCH Verlag GmbH & Co KGaA, Weinheim, Germany, 2010.
12 (*a*) C. E. MacBeth, A. P. Golombek, V. G. Young Jr., C. Yang, K. Kuczera, M. P. Hendrich and A. S. Borovik, *Science*, 2000, **289**, 938–941; (*b*) R. L. Shook, S. M. Peterson, J. Greaves, C. Moore, A. L. Rheingold and A. S. Borovik, *J. Am. Chem. Soc.*, 2011, **133**, 5810–5817; (*c*) W. Nam, *Acc. Chem. Res.*, 2015, **48**, 2415–2423; (*d*) K. Ray, F. F. Pfaff, B. Wang and W. Nam, *J. Am. Chem. Soc.*, 2014, **136**, 13942–13958.
13 H. Arzoumanian, J. F. Petrignani, M. Pierrot, F. Ridouane and J. Sanchez, *Inorg. Chem.*, 1988, **27**, 3377–3381.
14 (*a*) J. Tachibana, T. Imamura and Y. Sasaki, *J. Chem. Soc., Chem. Commun.*, 1993, 1436–1438; (*b*) M. Minato, D.-Y. Zhou, K.-i. Sumiura, Y. Oshima, S. Mine, T. Ito, M. Kakeya, K. Hoshino, T. Asaeda, T. Nakada and K. Osakada, *Organometallics*, 2012, **31**, 4941–4949.
15 G. Lyashenko, G. Saischek, A. Pal, R. Herbst-Irmer and N. C. Mösch-Zanetti, *Chem. Commun.*, 2007, 701–703.
16 A. Dupé, M. E. Judmaier, F. Belaj, K. Zangger and N. C. Mösch-Zanetti, *Dalton Trans.*, 2015, **44**, 20514–20522.
17 (*a*) C. Y. Lorber, S. P. Smidt and J. A. Osborn, *Eur. J. Inorg. Chem.*, 2000, 655–658; (*b*) S. N. Rao, N. Kathale, N. N. Rao and K. N. Munshi, *Inorg. Chim. Acta*, 2007, **360**, 4010–4016; (*c*) M. A. Katkar, S. N. Rao and H. D. Juneja, *RSC Adv.*, 2012, **2**, 8071.
18 H. Audouin, R. Bellini, L. Magna, N. Mézailles and H. Olivier-Bourbigou, *Eur. J. Inorg. Chem.*, 2015, **2015**, 5272–5280.
19 G. Alesso, M. Sanz, M. E. G. Mosquera and T. Cuenca, *Eur. J. Inorg. Chem.*, 2008, **2008**, 4638–4649.
20 H. Gehrke and J. Veal, *Inorg. Chim. Acta*, 1969, **3**, 623–627.
21 T. Robin, F. Montilla, A. Galindo, C. Ruiz and J. Hartmann, *Polyhedron*, 1999, **18**, 1485–1490.
22 N. Zwettler, J. A. Schachner, F. Belaj and N. C. Mösch-Zanetti, *Inorg. Chem.*, 2016, **55**, 5973–5982.
23 J. Leppin, C. Förster and K. Heinze, *Inorg. Chem.*, 2014, **53**, 1039–1047.
24 J. M. Mayer, *Inorg. Chem.*, 1988, **27**, 3899–3903.
25 (*a*) R. D. Rogers, E. Carmona, A. Galindo, J. L. Atwood and L. G. Canada, *J. Organomet. Chem.*, 1984, **277**, 403–415; (*b*) K. Most, J. Hoßbach, D. Vidović, J. Magull and

N. C. Mösch-Zanetti, *Adv. Synth. Catal.*, 2005, **347**, 463–472; (*c*) K. Hüttinger, C. Förster, T. Bund, D. Hinderberger and K. Heinze, *Inorg. Chem.*, 2012, **51**, 4180–4192.

26 (*a*) A. B. Blake, F. A. Cotton and J. S. Wood, *J. Am. Chem. Soc.*, 1964, **86**, 3024–3031; (*b*) B. Modec, M. Šala and R. Clérac, *Eur. J. Inorg. Chem.*, 2010, **2010**, 542–553; (*c*) M. M. El-Essawi, F. Weller, K. Stahl, M. Kersting and K. Dehnicke, *Z. Anorg. Allg. Chem.*, 1986, **542**, 175–181; (*d*) J. Leppin, C. Förster and K. Heinze, *Inorg. Chem.*, 2014, **53**, 12416–12427.

27 G. M. Sheldrick, *Acta Crystallogr., Sect. A: Fundam. Crystallogr.*, 2008, **64**, 112–122.